APPLICATION OF A MODEL UPDATING METHOD TO AN AIRCRAFT LONGITUDINAL STABILITY AUGMENTATION SYSTEM

Wellington S. Mattos , Natanael C. Pereira , Paulo C. Greco Jr.
University of Sao Paulo, Brazil

Keywords: *Aircraft Model Updating, Stability Augmentation System, Sensitivity Analysis*

Abstract

This paper describes the application of a model updating method, using experimental wind tunnel data, to an aircraft with a longitudinal stability augmentation system (LSAS). The aircraft model static stability margin could be adjusted by changing the center of rotation position which, in turn, coincided with the aircraft center of gravity position through weight balance. The study includes the development of the aircraft mathematical model, the description of an aircraft LSAS wind tunnel testing, the optimization using a mathematical tool to adjust aircraft and LSAS parameters such as stability derivatives, digital filter, sensor and servo dynamics. A parametric sensitivity analysis method was chosen for model updating. The optimization objective function is based on the difference between experimental and numerical pitch angle time response to a pulse canard deflection input. Three center of gravity positions are analyzed, one for which the aircraft is statically stable and two for which it is unstable. Results show large variations among adjusted parameters indicating the need for improvements in the implementation of the adopted numerical and experimental methodologies.

1 Introduction

A stability augmentation system (SAS) is an automatic flight control system that provides artificial stability to aircraft with undesirable flight characteristics [5]. The mathematical model for an aircraft with forward swept wing and canard is adjusted using experimental data obtained from wind tunnel tests. Frequency response experiments were conducted to estimate the servo-actuator transfer function. A model updating methodology was developed using optimization by sensitivity analysis.

The methodology was implemented in the commercial software Matlab environment using a computational model which included the aircraft and servo-actuator dynamics and the stability augmentation system using a PID controller [6]. The simulations were carried out for three center of gravity positions. The aircraft neutral point position was estimated from the open loop model and that value was kept constant for the closed loop model analysis. The closed loop model was adjusted for the three CG positions using the open loop results as initial values and using PID gain values corresponding to those of the wind tunnel experimental data.

The objective of this work is to compare the experimental results for three center of gravity positions [4] and for several PID gain values with the computational simulation results using the mathematical model with adjusted parameters. The results should validate the mathematical model, which can then be used to efficiently implement and test automatic control systems. The objective is to create means for testing methodologies for SAS development. There was no intention to reproduce real flight conditions.

Of the three CG positions, one, at 601 mm

from the aircraft nose, produced a statically stable airplane on the longitudinal plane and the other two, at 615 and 625 mm from the aircraft nose, produced a statically unstable airplane. The 601 mm CG position was just ahead of the neutral point making the airplane marginally stable. An airplane mathematical model was developed for the three center of gravity positions and put in transfer function format. Only the stable 601mm CG position was simulated with open loop. All three CG positions were tested with closed loop. The closed loop mathematical model included the PID, servo, sensor and digital filter dynamics. Servo and sensor dynamics were obtained from frequency domain experimental analysis for several servo/sensor amplitude values (5º, 10º, 15º, 20º and 25º). Characterization was based on measured cutoff frequency with an assumed ideal damping ratio of 0.707.

2 Characterization of Control System Dynamics

The block diagram of the aircraft with the LSAS is shown in Fig.1. An experimental analysis with the two servo-actuators was carried out with the objective of obtaining a representative transfer function. The tests were implemented with the

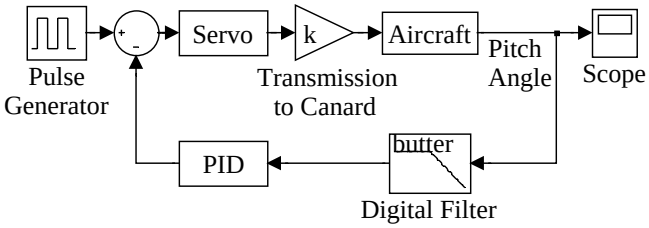

Fig. 1 Block diagram of the aircraft model with the LSAS.

aid of a data acquisition board connected to the sensors (precision potentiometers) and the actuators (aircraft model servos), used for canard deflection (Fig.2). The control system was the same used in a previous wind tunnel testing study [6]. This analysis aimed at obtaining the servo-actuator dynamic characteristics for the transfer function representation.

A sinusoidal input was given to the potentiometer by a motor. The potentiometer signal was sent to the control board where it went through a digital filter and the through the PID controller. The output signal is then sent to the servo-actuator. The servo rotation angle was read by a precision potentiometer. The input frequency range was from 0.1 to 3 Hz for the amplitude values of 5º, 10º, 15º, 20º and 25º. The servo output was recorded and processed to obtain the control system amplitude ratio (attenuation) and lag (phase angle). The frequency range was limited to 3 Hz to avoid damaging the servo. Two servos, with different maximum torque and speed characteristics, were tested. The lower torque servo (servo-actuator 1) presented good behavior throughout the test (Fig.3), but with a lower cutoff frequency of 3.4 Hz (slower response). The response has a second order transfer function behavior since phase angle is 90º at the cutoff frequency. The second servo-actuator (higher torque), presented a higher cutoff frequency of 5.5 Hz, and less variation between different amplitudes(Fig.4). That indicates higher precision and faster response than servo-actuator 1 but large deviation above the cutoff frequency indicate lower maximum operating frequency.

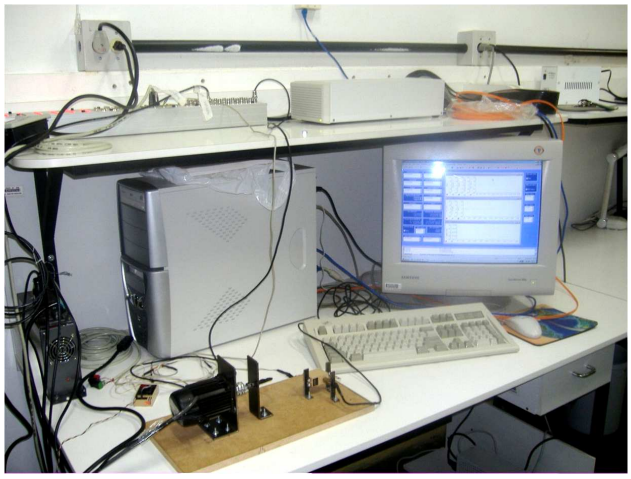

Fig. 2 Experimental setup for testing the control system servos, sensors and digital filter.

Servo frequency response function is defined by

$$\frac{x}{A}(\omega) = \frac{1}{1+2\zeta\left(\frac{\omega}{\omega_c}\right)i-\left(\frac{\omega}{\omega_c}\right)^2} \qquad (1)$$

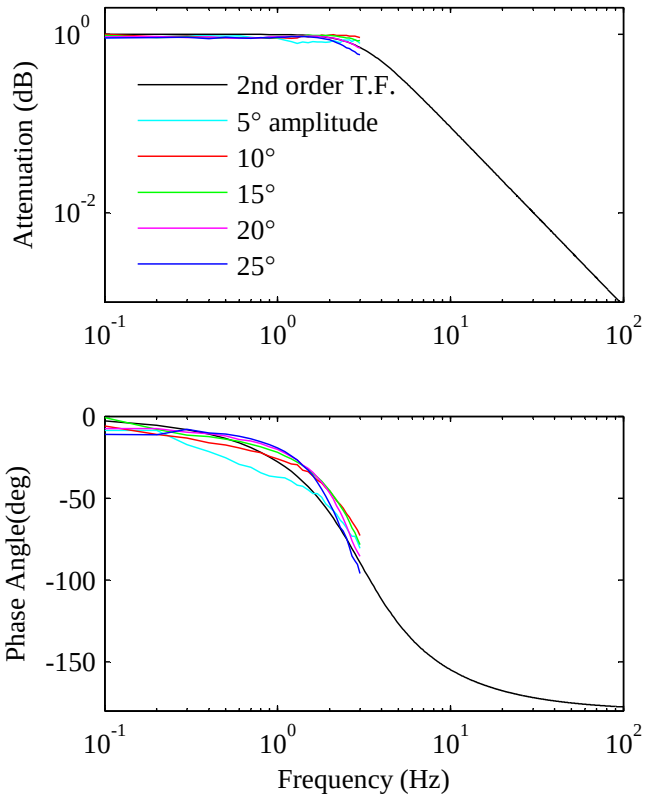

Fig. 3 Frequency response of servo-actuator 1 (Lower Torque) and adjusted 2nd order transfer function.

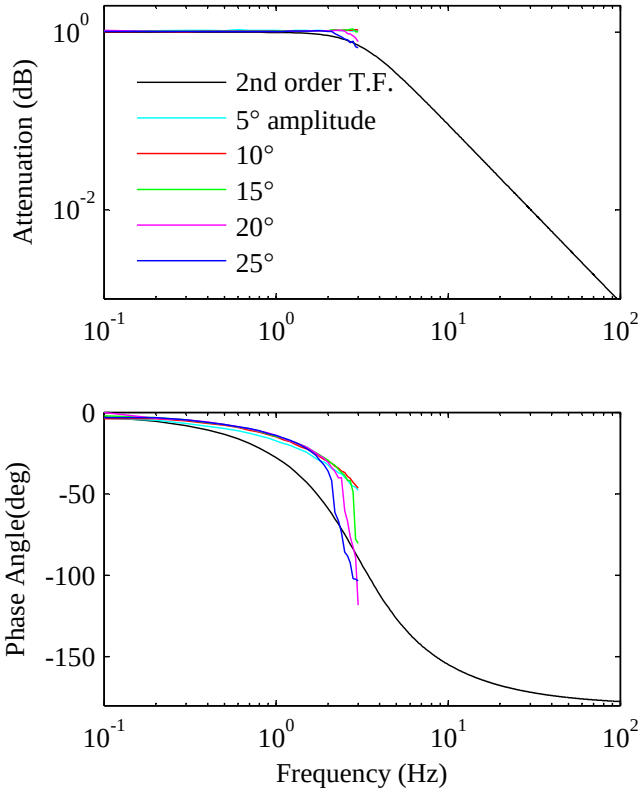

Fig. 4 Frequency response of servo-actuator 2 (Higher Torque) and adjusted 2nd order transfer function.

where ω_c is the cutoff frequency and ζ is the damping ratio.

The digital filter (low pass Butterworth) was implemented with an 8th degree transfer function with a cutoff frequency of 5 Hz. The precision potentiometer transfer function was a simple gain since the experiments showed no other significant effect for that sensor. The PID controller was adjusted with several gain combinations which gave good stability behavior to the model. The aircraft derivatives were estimated first order theoretical methods.

The aircraft one degree-of-freedom longitudinal equation of motion is given by

$$\frac{\theta}{\delta_c}(S) = \frac{M_{\delta_c}}{S^2 - M_q S - M_\alpha} \qquad (2)$$

where the derivatives were estimated using first order theoretical methods [8],[7]. Servo (canard actuator), potentiometer (pitch angle sensor) and a gimbal type mechanism were installed inside

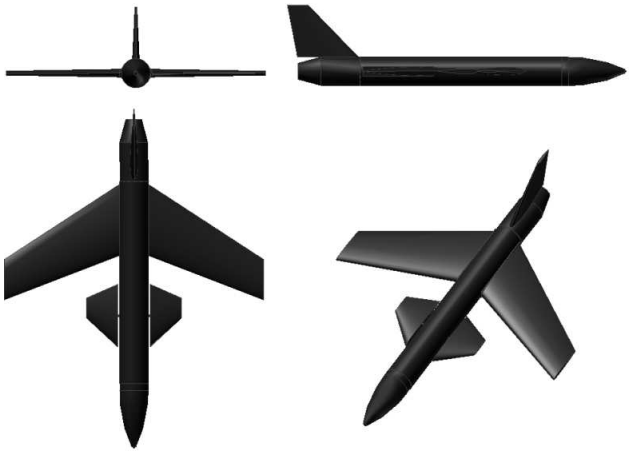

Fig. 5 Views of the aircraft model tested in the wind tunnel [6].

the fuselage. The basic aircraft model data is presented on Table1.

The model is fixed in the wind tunnel through a gimbal type mechanism which allows four degrees of freedom: pitch, yaw, roll, and climb. Each degree of freedom can be individually con-

Table 1 Model aircraft specifications.

FUSELAGE	
Length (m)	1.13
Diameter (m)	0.10
WING	
Reference area (m^2)	0.17
Span (m)	0.91
Mean aerodynamic chord (m)	0.20
Root chord (m)	0.24
Aspect ratio	4.8
Leading edge sweep	-20^o
Quarter chord sweep	-23^o
Taper ratio	0.60
Dihedral angle	0^o
Aileron area (m^2)	0.009
VERTICAL TAIL	
Reference area (m^2)	0.02
Mean aerodynamic chord (m)	0.14
Root chord (m)	0.20
Aspect ratio	1.4
Leading edge sweep	43^o
Quarter chord sweep	37^o
Taper ratio	0.33
Rudder area (m^2)	0.006
CANARD	
Reference area (m^2)	0.05
Span (m)	0.32
Mean aerodynamic chord (m)	0.19
Aspect ratio	1.9
Leading edge sweep	43^o
Quarter chord sweep	30^o
Taper ratio	0.22
Dihedral angle	0^o

strained. An extension tube attached the mechanism main axle to the wind tunnel bottom wall. The gimbal position along the x-axis is adjustable allowing modification of the C.G. position and, consequently, of model stability characteristics. The angular motions of gimbal mechanism are limited in $\pm 15^o$.

The control surfaces are commanded through servo-actuators and a precision potentiometer, attached to the rotation axle of the gimbal mechanism, was used to measure the pitch angle. One servo controls both sides of the canard in symmetrical motion.

A DSpace data acquisition system was used to measure the potentiometer signal and to implement the automatic control system and to control the servo-actuator.

The wind tunnel used in the experiments has a test section 1.7 m wide, 1.4 m high and 3 m long. It is a closed circuit wind tunnel with maximum velocity of about 50 m/s and turbulence level of 0.25% [2].

The experimental procedure consisted of installing the model inside the wind tunnel with the gimbal mechanism and placing the model with the desired CG position for weight balance [6]. In this paper the results for three CG positions are shown. Figure 6 shows the experimental setup in the wind tunnel.

Fig. 6 Wind tunnel setup with the research base aircraft model [6].

In the experiments, pitch and yaw degrees of freedom are unconstrained. Yaw motion is used only to trim the model, with the rudder, for directional motion to correct eventual asymmetries. In all tests wind tunnel velocity was set to 15 m/s. The parameters of the PID controller were estimated using a frequency response method developed by Ziegler-Nichols [1] mainly to determine a critical proportional gain K_{cr}.

3 Methodology

A parametric sensitivity analysis was used for optimal model updating [9]. The sensitivity analysis technique applied in the present work is based on Fiacco's Theorem [3]. System optimization is carried out adjusting key parameters searching for the best correlation possible between numerical and experimental results. The adjusted parameters for the stable open loop system (CG position at 601 mm) are:

1. Lift curve slope ($C_{L\alpha}$).
2. Variation of pitching moment coefficient with pitch rate (C_{Mq}).
3. Moment of inertia about the y axis (I_{yy}).
4. Aircraft neutral point position ($\bar{x}_{NP}$).

For the closed loop system three CG positions (601mm / 615 mm / 625 mm) are investigated with five parameters to be adjusted:

1. Lift curve slope ($C_{L\alpha}$).
2. Variation of pitching moment coefficient with pitch rate (C_{Mq}).
3. Moment of inertia about the y axis (I_{yy}).
4. Servo actuator cutoff frequency (ω_{servo}).
5. Servo actuator damping ratio (ζ_{servo}).

Minimization of a cost function

$$F = F(X_1, X_2, ..., X_n) \tag{3}$$

is obtained from a Taylor series expansion of the cost function gradient

$$\frac{\partial F}{\partial X_i} = \frac{\partial F^*}{\partial X_i} + \sum_j \frac{\partial^2 F^*}{\partial X_i \partial X_j} \Delta X_j + ... \tag{4}$$

or, considering that a minimum can be reached by the perturbation,

$$\sum_j \frac{\partial^2 F^*}{\partial X_i \partial X_j} \Delta X_j = -\frac{\partial F^*}{\partial X_i} \tag{5}$$

Wind tunnel was set with velocity of 15 m/s for CG-1 position. The parameters of the PID controller were estimated using a frequency response method developed by Ziegler-Nichols [10] mainly to determine a critical proportional gain, K_{cr}. Starting from that estimate, several tests were carried out modifying the PID controller parameters. The proportional and derivative gains are held fixed while the integral gain is varied from 0.0 to 2.0. This process is repeated for derivative gains going from 1.0 to 3.0 and, then, for proportional gains going from 11 to 15. In all cases gain increment was interrupted if the aircraft became unstable or if the canard became unresponsive due to servomotor limitations. This PID tunning procedure was carried out aiming at obtaining an efficient controller requiring reasonably small canard deflections.

4 Results and Analysis

The cost function was defined with the difference between numerical and experimental pitch angle response to a canard pulse perturbation:

$$F = \sqrt{\sum_t (\theta_{exp} - \theta_{num})^2} \tag{6}$$

Table 2 shows the results for center of gravity position 1 (601 mm from aircraft nose) with open loop that served as basis for the closed loop simulations and where the neutral point position was determined after adjustment using the experimental data.

Table 2 Results of simulation for open loop for position CG 601 mm from the nose of the model aircraft (stable position).

OPEN LOOP - CG 601 mm			
Variable Parameter	Initial Value	Adjusted Value	Relative Variation
$C_{L\alpha}$	4.7	3.8	20%
C_{Mq}	-3.4	-4.9	44%
I_{yy} (kg m^2)	0.16	0.12	25%
$\bar{x}_{np}$	-0.12	-0.12	0%

Considering center of gravity position 1 with closed loop, Tables 3 to 5 show adjusted $C_{L\alpha}$ in the range of 5% variation compared with the initial theoretical value of 4.7. The neutral point po-

sition was kept fixed in closed loop adjustment for all CG positions.

Figures 7 to 9, for center of gravity position 1, show that the numerical simulations do not reproduce the residual oscillations after the model stabilizes around the zero incidence angle. Those oscillations probably result from wind tunnel disturbances which are not included in the numerical model.

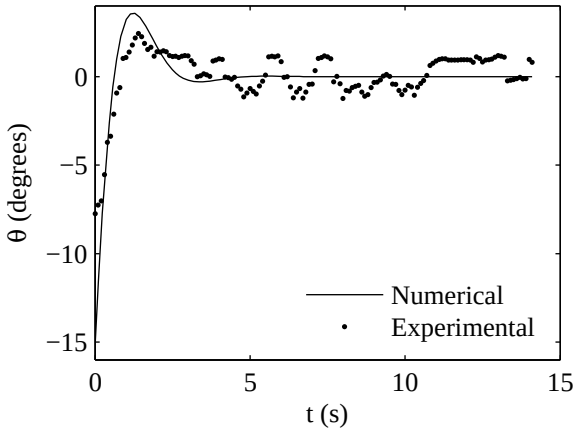

Fig. 7 Comparison between experimental and adjusted computational model results with CG 601 mm, P = 0.3, I = 0.0, D = 0.01.

Table 3 Results of simulation for closed loop for position CG 601 mm from the nose of the model aircraft (stable position).

CLOSED LOOP - CG 601 mm P = 0.3, I = 0.0, D = 0.01			
Variable Parameter	Initial Value	Adjusted Value	Relative Variation
$C_{L\alpha}$	4.7	4.4	6%
C_{Mq}	-3.4	-5.4	59%
I_{yy} (kg m^2)	0.16	0.07	56%
ω_{servo} (rad/s)	21	21	0%
ζ_{servo}	0.71	0.54	24%

Figures 10 to 12 and 13 to 16, show worse agreement with the experimental results specially near the overshoot but with reasonable correlation for the last two results.

During testing with the 615mm CG position it was noted that insertion of the filter did not

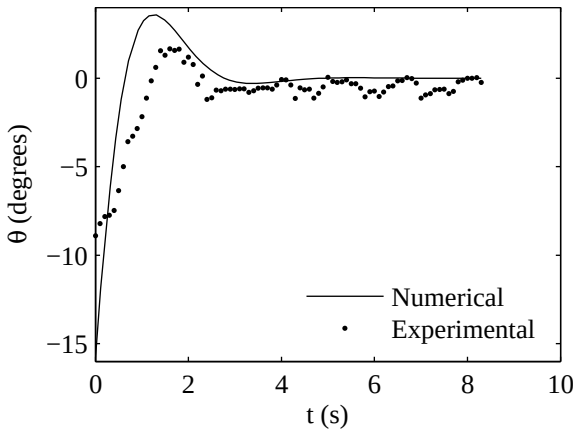

Fig. 8 Comparison between experimental and adjusted computational model results with CG 601 mm, P = 0.3, I = 0.0, D = 0.03.

influence aircraft stabilization in the simulations but, to a certain extent, it influenced the convergence of the model adjustment process. When the filter was replaced by a 10% gain (to reproduce the signal attenuation effect) the simulated aircraft system became unstable. It must be noted that there was no intention of reproducing a real flight condition but, even for the simplified wind tunnel model, many physical properties were not represented in the computational model.

In the wind tunnel, the aircraft model is fixed with an apparatus which include cables and wires that can affect damping and stiffness behavior and which were not included in the computational model. In the experimental results the dig-

Table 4 Results of simulation for closed loop for position CG 601 mm from the nose of the model aircraft (stable position).

CLOSED LOOP - CG 601 mm P = 0.3, I = 0.0, D = 0.03			
Variable Parameter	Initial Value	Adjusted Value	Relative Variation
$C_{L\alpha}$	4.7	4.2	11%
C_{Mq}	-3.4	-5.3	58%
I_{yy} (kg m^2)	0.16	0.07	50%
ω_{servo} (rad/s)	21	21	0%
ζ_{servo}	0.71	0.44	24%

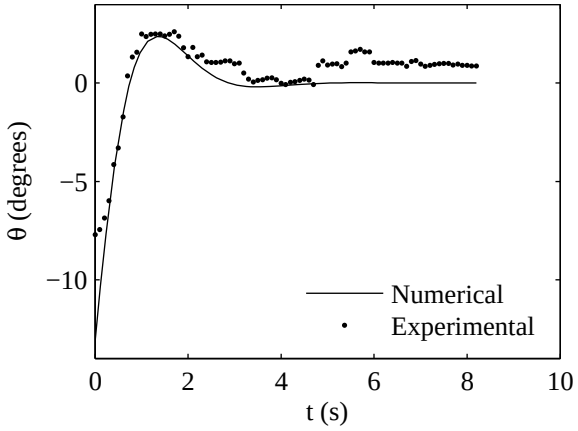

Fig. 9 Comparison between experimental and adjusted computational model results with CG 601 mm, P = 0.5, I = 0.04, D = 0.04.

ital filter produced high attenuation of the signal and required a corresponding increase in the PID gains. The computational model, which included the digital filter transfer function, presented almost no attenuation.

The use of more parameters for model adjustment could improve the results at the cost of increasing of simulation time. In most cases the experimental model stabilized at a pitch angle in a $\pm 2{,}5^{o}$ margin. The theoretical model could not reproduce the residual oscillations of the experimental data which are probably due to small wind tunnel random disturbances.

For the other two CG positions (615 and 625mm), which are aft of the neutral point (unstable positions), the adjusted parameters stayed within a reasonable range of variation for the data samples shown in the figures. Several other analyzed data samples resulted in larger variations and were discarded from the model adjustment process. Adjusted $C_{L\alpha}$ show less variation, with respect to the estimated theoretical value, than adjusted C_{Mq} values, as shown on Tables 6 to 11. This is consistent with the expected accuracy for first order theoretical estimations which is of around 10% for $C_{L\alpha}$ but only 20% for C_{Mq}.

Table 5 Results of simulation for closed loop for position CG 601 mm from the nose of the model aircraft (stable position).

CLOSED LOOP - CG 601 mm P = 0.5, I = 0.04, D = 0.04			
Variable Parameter	Initial Value	Adjusted Value	Relative Variation
$C_{L\alpha}$	4.7	4.3	9%
C_{Mq}	-3.4	-5.2	54%
I_{yy} (kg m^2)	0.16	0.05	30%
ω_{servo} (rad/s)	21	21	0%
ζ_{servo}	0.71	0.47	33%

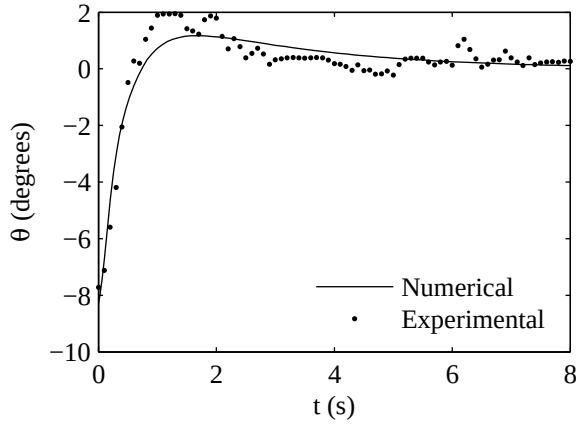

Fig. 10 Comparison between experimental and adjusted computational model results with CG 615 mm, P = 13, I = 1.6, D = 2.5.

Table 6 Results of simulation for closed loop for position CG 615 mm from the nose of the model aircraft (unstable position).

CLOSED LOOP - CG 615 mm P = 13, I = 1.6, D = 2.5			
Variable Parameter	Initial Value	Adjusted Value	Relative Variation
$C_{L\alpha}$	4.7	6.1	30%
C_{Mq}	-3.2	-3.2	0%
I_{yy} (kg m^2)	0.18	0.10	44%
ω_{servo} (rad/s)	21	23	10%
ζ_{servo}	0.71	0.71	0%

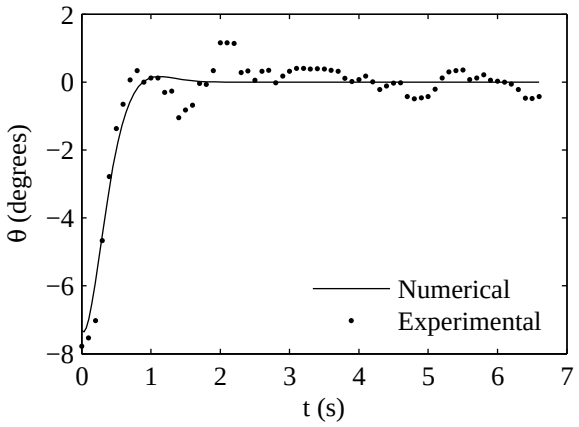

Fig. 11 Comparison between experimental and adjusted computational model results with CG 615 mm, P = 15, I = 0.0, D = 3.0.

Table 7 Results of simulation for closed loop for position CG 615 mm from the nose of the model aircraft (unstable position).

CLOSED LOOP - CG 615 mm P = 15, I = 0.0, D = 3.0			
Variable Parameter	Initial Value	Adjusted Value	Relative Variation
$C_{L\alpha}$	4.7	6.2	32%
C_{Mq}	-3.2	-3.7	16%
I_{yy} (kg m^2)	0.18	0.24	33%
ω_{servo} (rad/s)	21	22	5%
ζ_{servo}	0.71	0.73	3%

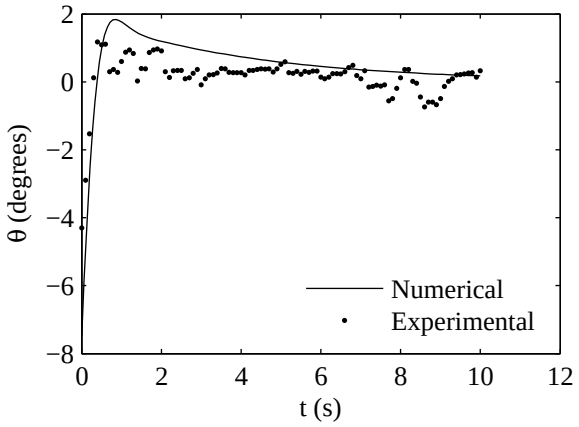

Fig. 12 Comparison between experimental and adjusted computational model results with CG 615 mm, P = 15, I = 1.6, D = 3.0.

Table 8 Results of simulation for closed loop for position CG 615 mm from the nose of the model aircraft (unstable position).

CLOSED LOOP - CG 615 mm P = 15, I = 1.6, D = 3.0			
Variable Parameter	Initial Value	Adjusted Value	Relative Variation
$C_{L\alpha}$	4.7	5.6	19%
C_{Mq}	-3.2	-3.7	16%
I_{yy} (kg m^2)	0.18	0.18	0%
ω_{servo} (rad/s)	21	22	5%
ζ_{servo}	0.71	0.71	0%

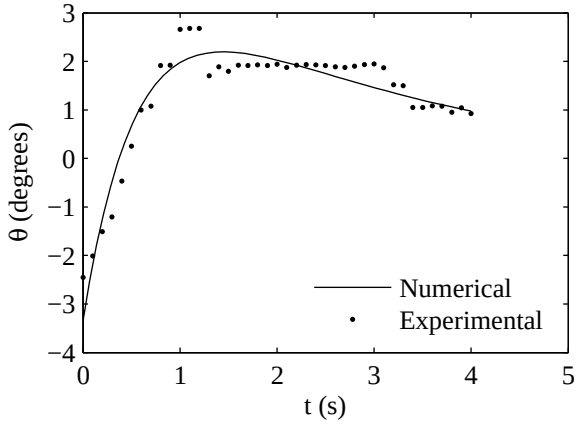

Fig. 13 Comparison between experimental and adjusted computational model results with CG 625 mm, P = 12, I = 1.6, D = 3.0.

Table 9 Results of simulation for closed loop for position CG 625 mm from the nose of the model aircraft (unstable position).

CLOSED LOOP - CG 625 mm P = 12, I = 1.6, D = 3.0			
Variable Parameter	Initial Value	Adjusted Value	Relative Variation
$C_{L\alpha}$	4.7	5.2	11%
C_{Mq}	-3.1	-4.4	42%
I_{yy} (kg m^2)	0.19	0.18	5%
ω_{servo} (rad/s)	21	22	5%
ζ_{servo}	0.71	0.70	1%

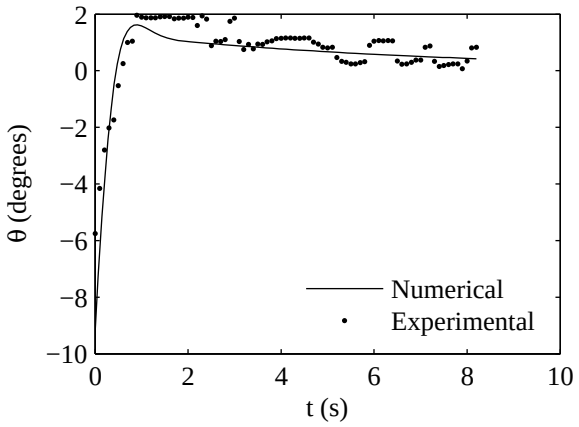

Fig. 14 Comparison between experimental and adjusted computational model results with CG 625 mm, P = 13, I = 0.8, D = 2.5.

Table 10 Results of simulation for closed loop for position CG 625 mm from the nose of the model aircraft (unstable position).

CLOSED LOOP - CG 625 mm P = 13, I = 0.8, D = 2.5			
Variable Parameter	Initial Value	Adjusted Value	Relative Variation
$C_{L\alpha}$	4.7	6.0	28%
C_{Mq}	-3.1	-3.6	16%
I_{yy} (kg m^2)	0.19	0.16	16%
ω_{servo} (rad/s)	21	22	5%
ζ_{servo}	0.71	0.65	8%

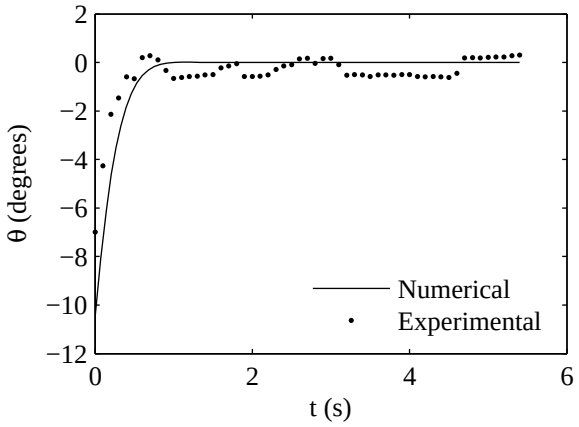

Fig. 15 Comparison between experimental and adjusted computational model results with CG 625 mm, P = 14, I = 0.0, D = 3.0.

Table 11 Results of simulation for closed loop for position CG 625 mm from the nose of the model aircraft (unstable position).

CLOSED LOOP - CG 625 mm P = 14, I = 0.0, D = 3.0			
Variable Parameter	Initial Value	Adjusted Value	Relative Variation
$C_{L\alpha}$	4.7	4.9	4%
C_{Mq}	-3.1	-3.5	13%
I_{yy} (kg m^2)	0.19	0.17	11%
ω_{servo} (rad/s)	21	21	0%
ζ_{servo}	0.71	0.71	0%

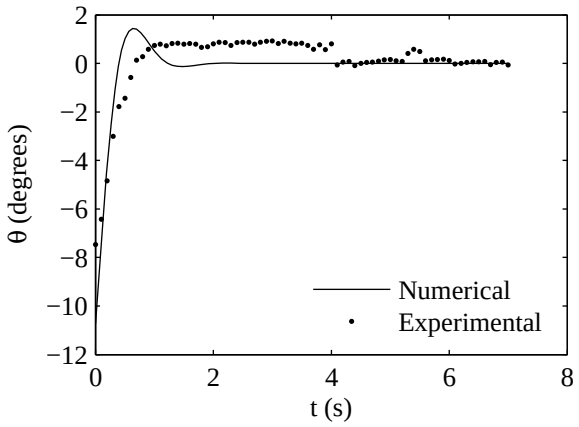

Fig. 16 Comparison between experimental and adjusted computational model results with CG 625 mm, P = 15, I = 0.0, D = 2.5.

Table 12 Results of simulation for closed loop for position CG 625 mm from the nose of the model aircraft (unstable position).

CLOSED LOOP - CG 625 mm P = 15, I = 0.0, D = 2.5			
Variable Parameter	Initial Value	Adjusted Value	Relative Variation
$C_{L\alpha}$	4.7	5.2	11%
C_{Mq}	-3.1	-3.8	23%
I_{yy} (kg m^2)	0.19	0.19	0%
ω_{servo} (rad/s)	21	22	5%
ζ_{servo}	0.71	0.52	27%

5 Conclusion

The adjusted theoretical model is useful for simulation of aircraft dynamics with low cost and reduced time, compared to a wind tunnel analysis. The adjusted results, based on wind tunnel experimental results with an inherently unstable aircraft model with LSAS, were satisfactory. That was possible despite the use of a simplified computational model generating adjusted results for open loop and closed loop systems for three positions of the center of gravity (the last two with negative static margin).

The parameters of the mathematical model started with first order theoretical approximations. The effect of cables in the wind tunnel fixture and fluctuations of wind tunnel flow, led to model stabilization at angles different from expected trim angle and with residual oscillations. That effect was not reproduced in the computational results. The experimental analysis used an 8^{th} order filter with cutoff frequency of 30 rad/s for the unstable CG positions. When the digital filter transfer function was included in the computational model it became unstable. It was necessary to remove the filter to obtain the desired stability. It is necessary to further investigate the filter influence and to improve the sensitivity analysis implementation to obtain better correlation between computational and experimental results.

6 Acknowledgments

The authors wish to thank CNPq for partially financing this work.

References

[1] Aström, K.. Hägglund, T.. *PID Controllers: Theory, Design and Tuning*, Instrumentation Systems and Automation Society, pp.135-138, 1995.

[2] Catalano. F. M.. "The new closed circuit wind tunnel of the aircraft laboratory of University of Sao Paulo", *Proceedings of the 16th Brazilian Congress of Mechanical Engineering*, 2001.

[3] Fiacco, A. V.. "'Sensitivity Analysis for nonlinear programming using penalty methods"', *Math Programming*, Vol. 10, No. 3, pp. 287-311, 1976.

[4] Mattos, W. S.. *Adjustment of an Aircraft Mathematical Model with Stability Augmentation System based on Wind Tunnel Analysis*. M.S. Thesis, Mechanical Engineering Dept., University of Sao Paulo, 2007.

[5] Nelson, R. C.. *Flight Stability and Automatic Control*, McGraw Hill, 1989.

[6] Pereira. N. C.. *Development of a Longitudinal Stability Augmentation System of a Forward Swept Wing and Canard Airplane with Wind Tunnel Testing*, M.S. Thesis, Mechanical Engineering Dept., University of Sao Paulo, 2005.

[7] Roskam, J.. *Aircraft Design - Part VI*, RAEC, 1987

[8] Roskam, J.. *Airplane Flight Dynamics and Automatic Flight Controls - Part I*. RAEC, 1979

[9] Sulieman, H., *Parametric Sensitivity Analysis in Non Linear Regression*, Ph.D. Thesis, Queen's University at Kingston, 1998.

[10] Voda, A. A., Landau, L. D.. A method for the auto-calibration of PID controllers, *Automatica*, Vol. 32, No. 1, pp. 41-53, 1995.

Copyright Statement